Stopped-Flow Kinetic Analysis of *Escherichia coli* Taurine/α-Ketoglutarate Dioxygenase: Interactions with α-Ketoglutarate, Taurine, and Oxygen†

Matthew J. Ryle, Raghavakaimal Padmakumar,‡ and Robert P. Hausinger*

Departments of Microbiology and Biochemistry, Michigan State University, East Lansing, Michigan 48824-1011

Received June 3, 1999; Revised Manuscript Received August 26, 1999

ABSTRACT: Taurine/α-ketoglutarate dioxygenase (TauD), a member of the broad class of non-heme Fe(II) oxygenases, converts taurine (2-aminoethanesulfonate) to sulfite and aminoacetaldehyde while decomposing α-ketoglutarate (αKG) to form succinate and CO_2. Under anaerobic conditions, the addition of αKG to Fe(II)TauD results in the formation of a broad absorption centered at 530 nm. On the basis of studies of other members of the αKG-dependent dioxygenase superfamily, we attribute this spectrum to metal chelation by the substrate C-1 carboxylate and C-2 carbonyl groups. Subsequent addition of taurine perturbs the spectrum to yield a 28% greater intensity, an absorption maximum at 520 nm, and distinct shoulders at 480 and 570 nm. This spectral change is specific to taurine and does not occur when 2-aminoethylphosphonate or *N*-phenyltaurine is added. Titration studies demonstrate that each TauD subunit binds a single molecule of Fe(II), αKG, and taurine. In addition, these studies indicate that the affinity of TauD for αKG is enhanced by the presence of taurine. α-Ketoadipate, the other α-keto acid previously shown to support TauD activity, and α-ketocaproate lead to the formation of weak 520 nm-like spectra with Fe(II)TauD in the presence of taurine; however, corresponding spectra at 530 nm are not observed in the absence of taurine. Pyruvate and α-ketoisovalerate fail to elicit absorption bands in this region of the spectrum, even in the presence of taurine. Stopped-flow UV−visible spectroscopy reveals that the 530 and 520 nm spectra associated with αKG−Fe(II)TauD and taurine−αKG−Fe(II)TauD are formed at catalytically competent rates (∼40 s^{-1}). The rate of chromophore formation was independent of substrate or enzyme concentration, suggesting that αKG binds to Fe(II)TauD prior to the formation of a chromophoric species. Significantly, the taurine−αKG−Fe(II)TauD state, but not the αKG−Fe(II)TauD species, reacts rapidly with oxygen (42 ± 9 s^{-1}). Using the data described herein, we develop a preliminary kinetic model for TauD catalysis.

Taurine/α-ketoglutarate (αKG)[1] dioxygenase (TauD) is an 81 kDa homodimer that catalyzes the conversion of taurine (2-aminoethanesulfonic acid) to sulfite and aminoacetaldehyde in the presence of oxygen, αKG, and Fe(II) as illustrated in Scheme 1 (*1*). The *Escherichia coli* enzyme is synthesized in response to sulfur starvation and allows the cell to utilize taurine as a sulfur source (*2*). Since taurine is the most abundant free intracellular amino acid in many tissues of humans and other animal species (*3*), large amounts are excreted into the environment, often in the form of bile salts (*4*). Taurine and other related sulfonates are the major sulfur compounds in forest soils (*5*); thus, sulfonates serve as an important source of sulfur for microorganisms.

Sequence analysis demonstrates a clear homology (30% sequence identity) between TauD and 2,4-dichlorophenoxyacetic acid (2,4-D)/αKG dioxygenase (TfdA), another biodegradative enzyme that catalyzes the first step in the degradation of the herbicide 2,4-D (Scheme 2) (*6*). Both enzymes couple the oxidative decarboxylation of αKG to succinate and CO_2 with the hydroxylation of substrate to form intermediates which spontaneously decompose to liberate useful metabolic precursors. TauD and TfdA define a separate subfamily of enzymes whose sequences are only slightly homologous to those of other mechanistically related αKG-dependent enzymes or alternative non-heme Fe(II) enzymes that activate dioxygen. Despite this sequence divergence, members of the enzyme superfamily are thought to utilize a similar mechanism to generate reactive oxygen intermediates; thus, kinetic and mechanistic studies of TauD

Scheme 1

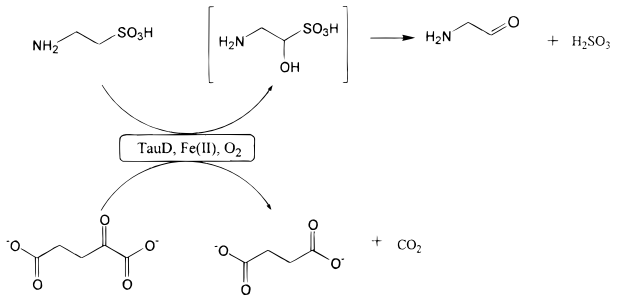

† This work was supported by NSF Grant MCB 9603520 and State of Michigan Research Excellence Funds.

* To whom correspondence should be addressed. Phone: (517) 353-9675. Fax: (517) 353-9857. E-mail: hausinge@pilot.msu.edu.

‡ Current address: Michigan Biotechnology Institute, 3900 Collins Rd., Lansing, MI 48909-0609.

[1] Abbreviations: αKG, α-ketoglutarate; TauD, taurine/αKG dioxygenase; Tris, tris(hydroxymethyl)aminomethane; EDTA, ethylenediaminetetraacetic acid; TE, 20 mM Tris buffer with 1 mM EDTA; MCD, magnetic circular dichroism; 2,4-D, 2,4-dichlorophenoxyacetic acid; TfdA, 2,4-D/αKG dioxygenase; DAOCS, deacetoxycephalosporin C synthase; CS, clavaminic acid synthase; IPNS, isopenicillin N synthase.

10.1021/bi9912746 CCC: $18.00
Published on Web 10/29/1999

Scheme 2

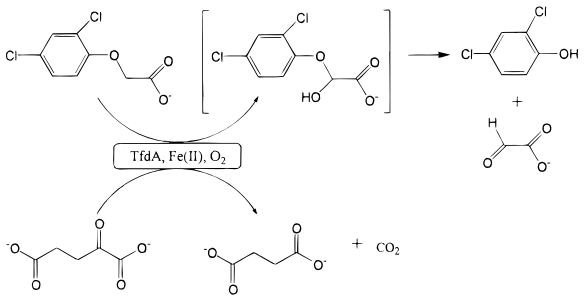

(and TfdA) are likely to provide insights into the broader groups of Fe(II) oxygenases.

Enzymes in the αKG-dependent dioxygenase superfamily catalyze a wide variety of biological oxidations (*7*, *8*). Several members carry out αKG-dependent hydroxylation reactions similar to those of TauD and TfdA. For example, prolyl hydroxylase post-translationally modifies prolyl residues during collagen biosynthesis (*9*). Similarly, other enzymes hydroxylate Lys or Asp/Asn residues or intermediate plant metabolites (*10*−*12*). Clavaminic acid synthase (CS) catalyzes three distinct chemical transformations (hydroxylation, ring formation, and desaturation) during the biosynthesis of the β-lactamase inhibitor clavulanic acid (*13*, *14*). Deacetoxycephalosporin C synthase (DAOCS) catalyzes the expansion of a five-membered thiazolidine ring into a six-membered dihydrothiazine ring (*15*). Although not requiring αKG, the ring-forming enzyme isopenicillin N synthase (IPNS) is also included in this group of Fe(II)-dependent catalysts (*16*). Many members of this superfamily possess a His-X-Asp-$X_{(\sim 55)}$-His motif (*17*). X-ray crystal structures of DAOCS and IPNS confirmed that the Asp and two His residues in this motif function as ligands to the metallocenter in these enzymes (*15*, *16*). Furthermore, mutagenesis studies are consistent with this assignment in the case of several hydroxylases (*10*−*12*, *18*, *19*), including TfdA.[2] More generally, a 2-His-1-carboxylate facial triad has been described as an emerging structural motif among non-heme Fe(II) enzymes (*20*). In the crystal structure of substrate-free DAOCS, solvent molecules occupy the remaining three coordination sites (*15*). Addition of αKG displaces two solvent ligands as it binds to the ferrous center via its C-1 carboxylate and C-2 carbonyl moieties (*15*). This mode of chelation was also proposed for αKG bound to CS on the basis of magnetic circular dichroism (MCD) spectroscopic evidence (*13*). Additional MCD studies of CS (*14*) suggest that upon binding the cosubstrate the ferrous center changes from a six-coordinate to a five-coordinate ligand environment. This change, possibly a common mechanistic attribute of this enzyme class, was proposed to create an O_2 binding site within the enzyme, but only when both substrates are bound. Crystallographic studies of IPNS are also consistent with the creation of an O_2 binding site upon substrate binding (*16*). The rates of formation of the supposed intermediates in these enzymes have not been addressed; thus, their catalytic competence is unknown.

Here the interactions of TauD with Fe(II), αKG, taurine, and oxygen are examined by electronic spectroscopy, including the use of stopped-flow methods. The data are incorporated into a preliminary kinetic model for the catalytic cycle of this αKG-dependent dioxygenase.

[2] With a more distant second His; D. A. Hogan, S. R. Smith, E. A. Saari, J. McCracken, and R. P. Hausinger, manuscript in preparation.

EXPERIMENTAL PROCEDURES

Purification of TauD. The gene encoding TauD was overexpressed from pME4141 (*1*) in *E. coli* BL21(DE3) cells. Ten-liter cultures of these cells were grown in LB medium at 30 °C, stirring at 300 rpm, with an air flow rate of 10 L/min using a Microferm fermentor (New Brunswick Instruments). When cultures reached an A_{600} of 0.4−0.7, *tauD* expression was induced by the addition of isopropyl β-D-thiogalactopyranoside to a final concentration of 1 mM. Cells were harvested after a 3 h induction period using a Pellicon Cassette System (Millipore) and pelleted by centrifugation for 10 min at 8000*g* and 4 °C. The cell pellet was resuspended in 100 mL of 20 mM Tris buffer (pH 7.7) with 1 mM EDTA (TE) and 20% glycerol. Aliquots (50 mL) were stored at −20 °C until they were needed.

Prior to lysis using a French pressure cell, 10 μg/mL DNase, 1.5 mM phenylmethanesulfonyl fluoride, and 0.01 mg/mL leupeptin were added to the thawed aliquots. The lysate was clarified by centrifugation for 45 min at 110000*g* and applied to a 2.5 cm × 30 cm Fast Flow DEAE-Sepharose (Pharmacia) column. The column was rinsed with 1 column volume of TE buffer (pH 7.7) containing 20% glycerol and 50 mM NaCl, and eluted using a linear 800 mL gradient from 50 to 300 mM NaCl in the same buffer at a flow rate of 5 mL/min. Fractions containing TauD were concentrated to 100 mL in a Millipore stirred cell concentrator with a YM 30 membrane. The concentrated eluant was loaded onto a 2.5 cm × 20 cm high-performance Q-Sepharose (Pharmacia) column equilibrated with TE buffer (pH 7.7) containing 20% glycerol and 50 mM NaCl. Proteins were eluted with a 400 mL linear gradient from 50 to 250 mM NaCl in the same buffer at a flow rate of 3 mL/min. The TauD-containing fractions were concentrated and extensively dialyzed against 25 mM imidazole buffer (pH 7.0) containing 20% glycerol at 4 °C. The dialyzed protein was frozen at −20 °C.

Enzyme Assays. TauD activity was measured using Ellman's reagent as previously described (*1*), except that assays were carried out in 10 mM 3,3-dimethylglutaric acid buffer (pH 7.0). Protein concentrations were determined using a commercial protein assay (Bio-Rad) with standard curves determined using preweighed bovine serum albumin purchased from the same source. The TauD used in these studies had a specific activity ranging from 3.8 to 5.8 μmol of sulfite produced min^{-1} (mg of TauD)$^{-1}$.

Analysis of Fe(II), αKG, and Taurine Binding to TauD Using UV−*Visible Spectroscopy.* All stock solutions for UV−visible binding studies were prepared inside serum vials sealed with butyl rubber stoppers. Stock solutions (30 mM) of αKG and taurine were prepared in 25 mM imidazole buffer (pH 7.0), and made anaerobic by several rounds of vacuum degassing and flushing with argon using a vacuum manifold. After the stock solutions had been degassed, dithionite was added to a final concentration of 2 mM from a 100 mM stock solution. Ferrous ammonium sulfate stock solutions (30 mM) were prepared by several rounds of degassing and flushing with argon inside a sealed serum vial.

The Fe(II) salt was dissolved in the desired volume of 25 mM imidazole buffer (pH 7.0) containing 2 mM dithionite. TauD was made anaerobic by multiple rounds of degassing and flushing with argon and adjusted to 2 mM dithionite.

All equilibrium spectroscopic studies used a 1 cm path length, 2 mL quartz cuvette fitted with a stopper and purged with argon. TauD [0.5 mM subunit in 25 mM imidazole buffer (pH 7.0) containing 2 mM dithionite] was transferred into the cuvette using a gastight syringe (Hamilton) that had been flushed with 2 mM dithionite buffer. After blanking against TauD, we recorded spectra for samples to which anaerobic aliquots of Fe(II), αKG, or taurine had been added. No significant absorption between 400 and 700 nm was detected for TauD-free dithionite buffer containing Fe(II), αKG, and taurine [or for Fe(II) binding to TauD]. Saturation plots were obtained by plotting the 530 nm absorption for the αKG−Fe(II)TauD samples or the 520 nm absorption for the αKG−taurine−Fe(II)TauD samples versus the concentration of the added titrant. Stock solutions were prepared to minimize the dilution (<4%) that occurred due to aliquot addition. The titration data were fitted to eq 1

$$A_{obs} = A_{max}[E_L]/n[E_T] \quad (1)$$

in which the observed absorption (A_{obs}) was equal to the maximal absorption (A_{max}) times the concentration of the enzyme−ligand complex ([E_L]) divided by the concentration of ligand binding sites [the number (n) of ligands bound per subunit times the total enzyme subunit concentration ([E_T])]. The amount of enzyme−ligand complex was obtained using eq 2

$$[E_L] = \{(K_d + [L_T] + n[E_T]) \pm [(K_d + [L_T] + n[E_T])^2 - (4[L_T]n[E_T])]\}/2 \quad (2)$$

where K_d is the apparent ligand affinity and [L_T] the total ligand concentration. The values of n and the K_d were determined for eqs 1 and 2 by using a multivariable least-squares analysis (KaleidaGraph, Synergy Software, Reading, PA). The errors presented in the text represent the standard deviations from five independent experiments on three different protein preparations.

Stopped-Flow UV−Visible Spectroscopy. Stock chemical and enzyme solutions for stopped-flow spectroscopic measurements were prepared as described above. Stopped-flow studies were carried out using a 0.4 cm path length Olis RSM-16 UV−visible stopped-flow spectrophotometer, and the resulting data were processed using the Olis data package (version 1.98.9) or KaleidaGraph software. To carry out anaerobic measurements, the instrument was fitted with specially designed reservoirs that contained butyl rubber crimp seals on the top, stopcocks on the bottom, and ground glass syringe fittings to connect snugly on the instrument. These reservoirs were made anaerobic using a vacuum manifold, filled with 25 mM imidazole buffer (pH 7.0) containing 2 mM dithionite buffer, and used to purge the spectrophotometer. One reservoir was filled with 1 mM Fe(II)TauD containing 2 mM dithionite, while the other reservoir contained the indicated additives in the same buffer. Each syringe was flushed with six 100 μL volumes of the solutions. Four stopped injections were run prior to collecting data.

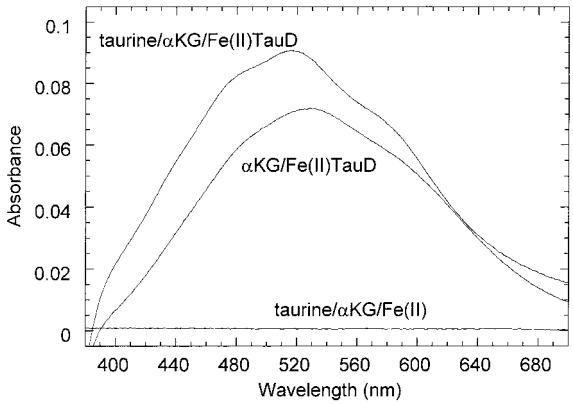

FIGURE 1: Difference absorption spectra of Fe(II)TauD in the presence of αKG and αKG−taurine. The anaerobic αKG−Fe(II)-TauD sample contained 0.5 mM TauD (subunit), 1.25 mM ferrous ammonium sulfate, 1.5 mM αKG, 25 mM imidazole buffer (pH 7.0), and 2 mM dithionite. The taurine−αKG−Fe(II)TauD spectrum was obtained after adding taurine (1.5 mM) to αKG−Fe(II)TauD. To highlight the features attributed to this weak chromophore, the spectrum of Fe(II)TauD was subtracted from the presented spectra.

For experiments where samples were reacted with oxygen, the instrument was made anaerobic in the described manner using 0.5 mM dithionite. Samples were prepared in 25 mM imidazole buffer (pH 7.0) containing 0.1−0.5 mM dithionite and the other components as indicated. The second syringe contained oxygen-saturated (purged with gas from an O_2 cylinder) 25 mM imidazole buffer (pH 7.0). On the basis of the stability of the colored samples, the reservoir cells and syringe maintained anaerobicity for at least 30 min.

RESULTS

Purification of TauD. Isopropyl β-D-thiogalactopyranoside-induced *E. coli* BL21(DE3)(pME4141) cells generated large amounts of the *tauD* product as previously described (*1*). A simple and rapid purification procedure provided homogeneous TauD (as monitored by Coomassie-stained SDS gels) with specific activities ranging from 3.8 to 5.8 μmol of sulfite formed min^{-1} (mg of TauD)$^{-1}$. Using the modified procedure, 300 mg of TauD could be purified from 5 L of fermentor-grown cells. The studies described below utilized more than 4 g of isolated enzyme.

αKG and Taurine Binding to Fe(II)TauD Monitored by UV−Visible Spectroscopy. Anaerobic addition of αKG to Fe(II)TauD resulted in a lilac-colored solution that yielded a broad absorption spectrum centered at 530 nm with an ϵ_{530} of 140 M^{-1} cm^{-1} (Figure 1). Subsequent binding of taurine to αKG−Fe(II)TauD caused a shift in the absorption maximum to 520 nm (ϵ_{520} = 180 M^{-1} cm^{-1}), and the spectrum exhibited more distinct features at 470 and 570 nm. No absorbance was observed in this region for taurine−Fe(II)TauD.

The effects of other α-keto acids on the Fe(II)TauD electronic spectrum were assessed (Figure 2). As shown in panel A, the addition of 5 mM pyruvate (trace 1), α-ketoisovalerate (trace 2), or α-ketocaproate (trace 3) to Fe(II)-TauD led to insignificant absorption increases in the 380−700 nm range. In contrast, α-ketoadipate (trace 4), the only other α-keto acid found to significantly support TauD activity (*1*), afforded a weak absorption increase with a maximum at 540 nm. The intensity of this absorption was 2% of that

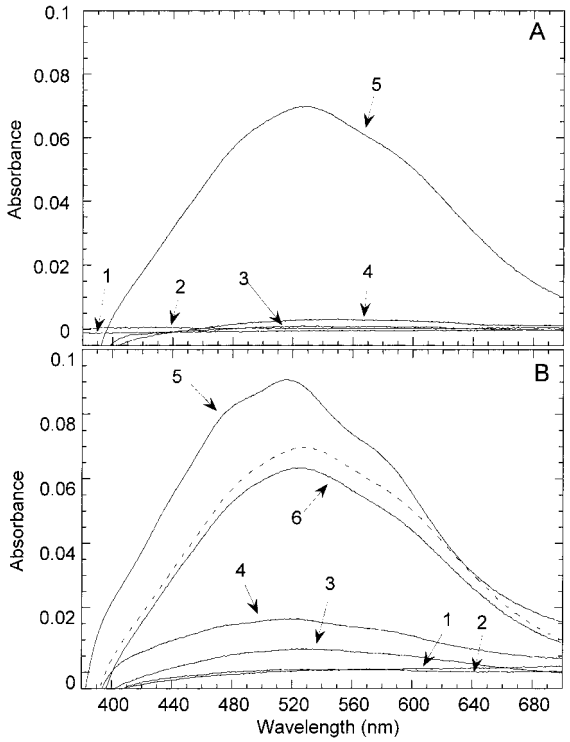

FIGURE 2: Difference absorption spectroscopic study of the interactions of Fe(II)TauD with substrate analogues. (A) Visible region absorption spectra of Fe(II)TauD (0.5 mM) with 5 mM pyruvate (trace 1), α-ketoisovalerate (trace 2), α-ketocaproate (trace 3), α-ketoadipate (trace 4), or αKG (trace 5). (B) Absorption spectra of the same samples in the presence of 2 mM taurine. Panel B also shows the absorption spectrum of the αKG−Fe(II)TauD complex in the presence of 5 mM 2-aminoethylphosphonic acid (trace 6). For comparison, the spectrum of αKG−Fe(II)TauD is reproduced as a dashed line. All samples were anaerobically prepared and contained 2 mM dithionite, 1.25 mM Fe(II), and 25 mM imidazole buffer (pH 7.0). The spectrum of Fe(II)TauD was subtracted from the presented spectra.

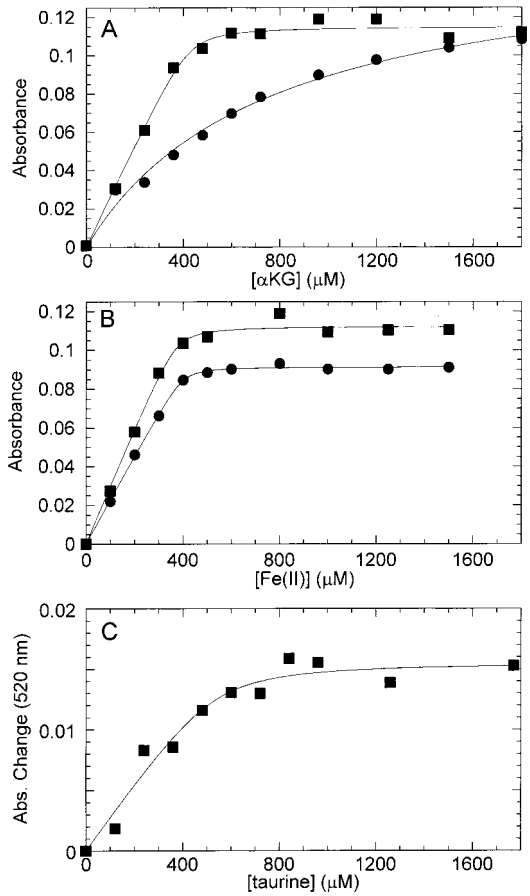

FIGURE 3: Dependence of chromophore formation on the concentration of Fe(II), αKG, or taurine. (A) The 530 nm absorption (●) associated with αKG−Fe(II)TauD and the 520 nm absorption (■) associated with taurine−αKG−Fe(II)TauD were monitored as a function of αKG concentration. (B) Absorption changes at 530 nm (●) associated with αKG−Fe(II)TauD and at 520 nm (■) associated with taurine−αKG−Fe(II)TauD were monitored as a function of Fe(II) concentration. (C) The change in spectral intensity at 520 nm (■) was followed upon addition of taurine to αKG−Fe(II)-TauD. All samples contained 0.5 mM TauD and 2 mM dithionite in 25 mM imidazole buffer (pH 7.0). When present at constant levels, the αKG, taurine, and Fe(II) were at concentrations of 2, 2, and 1.5 mM, respectively.

observed for enzyme in the presence of αKG (trace 5). Panel B presents the absorption spectra of Fe(II)TauD in the presence of these α-keto acids when taurine was added. Inclusion of taurine led to an increase in the intensity of the α-ketoadipate-associated spectrum (trace 4) and generated a spectrum for the sample containing α-ketocaproate (trace 3). Pyruvate (trace 1) and α-ketoisovalarate (trace 2) did not generate an absorbance spectrum characteristic of αKG binding in the presence of taurine. The absorption spectra for taurine−α-ketoadipate−Fe(II)TauD and taurine−α-ketocaproate−Fe(II)TauD were similar in shape to, but much less intense than (18 and 8%, respectively), the spectrum recorded for the taurine−αKG−Fe(II)TauD complex (trace 5) using identical concentrations of protein and reagents.

Two taurine analogues were examined for their ability to affect the αKG-associated absorbance spectrum. 2-Aminoethylphosphonic acid (the phosphonate analogue of taurine) failed to perturb the UV−visible spectrum of αKG−Fe(II)-TauD (Figure 2B, trace 6). Similarly, *N*-phenyltaurine (data not shown) also failed to induce the taurine-associated spectral changes. Neither of these taurine analogues is a substrate for the enzyme.

Stoichiometry of αKG, Fe(II), and Taurine Binding to TauD. Titration of αKG into a solution of Fe(II)TauD led to a progressive increase in absorbance at 530 nm, as illustrated in Figure 3A (●). Multivariable fitting of these titration data to eqs 1 and 2 suggested that the absorbance changes correlated with each TauD subunit binding 0.85 ± 0.05 αKG molecule with an apparent affinity of 350 ± 70 μM. Repetitive studies with multiple enzyme preparations yielded robust values for n of 0.9 ± 0.2 and for K_d of 270 ± 100 μM. Significantly, when the experiment was carried out in the presence of taurine, the stoichiometry of αKG binding remained unchanged, but the apparent affinity for αKG was increased to 6 ± 5 μM [panel A (■)]. The enhanced affinity for αKG was confirmed by additional studies (providing values for n of 0.83 ± 0.15 and for K_d of 20 ± 19 μM). To assess the Fe(II) concentration dependence of the chromophore, increasing concentrations of ferrous ammonium sulfate were titrated into solutions of αKG−TauD, with or without taurine (Figure 3B). Fitting of the data to eq 1 showed that in the absence (●) or presence (■) of taurine, TauD bound 0.75−0.80 Fe(II) molecule per subunit with high affinity (K_d < 8 μM). The stoichiometry of taurine binding to TauD was examined by monitoring the increase in spectral intensity at 520 nm as substrate was added to αKG−Fe(II)TauD (Figure 3C). The data were

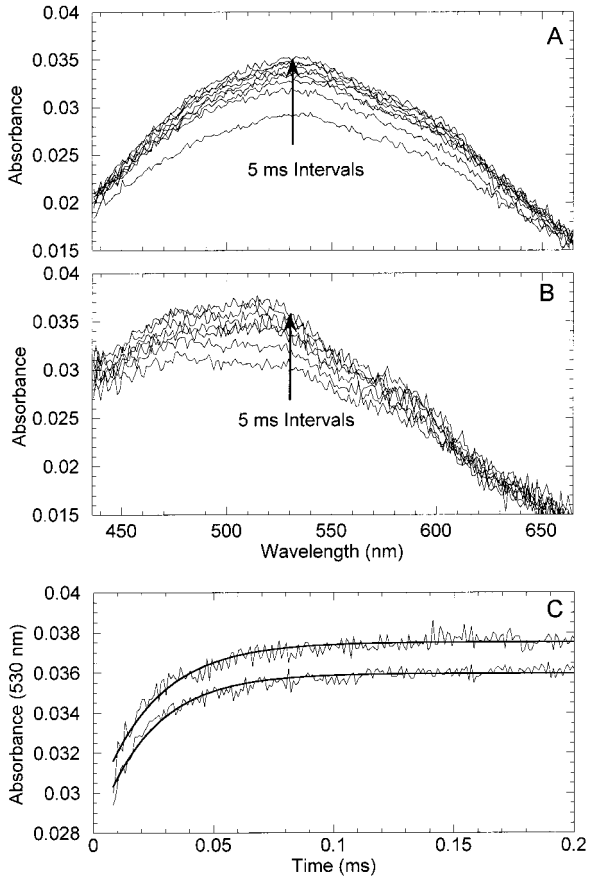

FIGURE 4: Rates of αKG−Fe(II)TauD and taurine−αKG−Fe(II)-TauD chromophore formation monitored by stopped-flow spectroscopy. (A) Absorption spectra resulting from a mixture of equal volumes of 1 mM Fe(II)TauD with 4 mM αKG. The least intense spectrum was collected immediately after mixing (7 ms), and the spectra with increasing intensities were recorded at 5 ms intervals. (B) Absorption spectra resulting from mixture of 1 mM Fe(II)-TauD with 4 mM taurine and 4 mM αKG. After mixing, the spectra with increasing intensities were recorded at 5 ms intervals. (C) The absorptions at 530 nm associated with αKG−Fe(II)TauD or taurine−αKG−Fe(II)TauD were recorded vs time. The data were fit to single-exponential processes (44 ± 2 s^{-1} for the former and 42 ± 3 s^{-1} for the latter). All solutions contained 2 mM dithionite in 25 mM imidazole buffer (pH 7.0).

consistent with 1.0 ± 0.2 molecules of taurine binding to each TauD subunit and an affinity of approximately 30 μM. In summary, each TauD subunit binds a single molecule of αKG, Fe(II), and taurine with high affinity.

Rate of Cosubstrate Binding to TauD Monitored by Stopped-Flow Spectroscopy. To establish whether the chromophores associated with αKG−Fe(II)TauD and taurine−αKG−Fe(II)TauD species were catalytically relevant, their rates of formation were examined by stopped-flow spectroscopy (Figure 4). Panel A shows the absorption spectra that developed upon mixing Fe(II)TauD with αKG in a 0.4 cm path length stopped-flow apparatus. Panel B shows results from an analogous experiment carried out with the added presence of taurine. In both cases, the chromophores were formed according to single-exponential processes for data collected between 8 and 200 ms [44 ± 2 s^{-1} for αKG−Fe(II)TauD and 42 ± 3 s^{-1} for taurine−αKG−Fe(II)TauD], as shown in panel C. At longer times (to 2 s), a slow increase in absorbance was observed that accounted for between 12 and 28% of the total absorbance change; we attribute this feature to the precipitation of protein in the stopped-flow cell. Rate information obtained from replicate experiments was more reproducible when the entire spectral change, from 436 to 665 nm, was fit using the single-exponential plus background fitting routine provided in the Olis software package (version 1.98.9). Table 1 presents the results from experiments where the rate dependence of chromophore formation on protein and substrate concentrations was investigated. In these studies, the substrate/enzyme ratio was varied from 0.5 to 8; examination of lower substrate concentrations was precluded by the low intensity of the signal. Unexpectedly, the spectrum of the αKG-bound state was found to be formed in a zero-order process that was independent of substrate or protein concentration. The presence of taurine had no effect on this rate. Since much of the reaction appeared to be completed within the instrument's mixing time, the concentration dependence of the rate of chromophore formation also was monitored at lower temperatures. At 4 °C, the fitting amplitudes were approximately 3 times that observed at room temperature, indicating that a larger proportion of the absorbance change was being observed, but protein precipitation was more of a problem. Nevertheless, the data demonstrated that the αKG−Fe(II)TauD and the taurine−αKG−Fe(II)TauD chromophores were formed with similar rates (4.4 ± 2.8 and 3.4 ± 1.9 s^{-1}, respectively) and that these rates were independent of substrate concentration (data not shown).

Table 1: Effect of Substrate and Enzyme Concentrations on the Rates of αKG−Fe(II)TauD or Taurine−αKG−Fe(II)TauD Chromophore Formation[a]

[αKG] (μM)	[taurine] (μM)	[Fe(II)TauD][b] (μM)	observed rate[c] (s^{-1})	trials[d]	preps[e]
250	−	250	48 ± 17	6	2
2000	−	250	42 ± 18	5	2
250	−	500	44 ± 11	6	3
500	−	500	47 ± 9	8	3
1000	−	500	39 ± 10	5	3
2000	−	500	44 ± 7	12	4
4000	−	500	39 ± 9	3	1
2000	250	500	39 ± 13	6	2
2000	1000	500	44 ± 8	7	2
2000	2000	500	40 ± 14	9	4

[a] Anaerobic solutions of Fe(II)TauD were mixed at room temperature with anaerobic substrate solutions using the indicated concentrations, and the spectroscopic changes were monitored over time in an Olis RSM-16 UV−visible stopped-flow spectrophotometer. [b] Subunit concentration. [c] Rates were obtained using the single-exponential global fitting routine provided in the Olis software package. Individual scans were fit from 7 to 200 ms. [d] Number of stopped-flow traces that were averaged to obtain the presented rates. [e] Number of independent protein preparations used for comparisons.

The rate of taurine binding to αKG−Fe(II)TauD was also examined by stopped-flow spectroscopy. Transformation of the αKG−Fe(II)TauD spectrum into the taurine−αKG−Fe(II)TauD spectrum (>140 s^{-1}) was complete within the 7 ms dead time of the instrument.

Oxygen Reactivity of the αKG−Fe(II)TauD and αKG−Taurine−Fe(II)TauD States. To assess the oxygen reactivity of αKG−Fe(II)TauD and taurine−αKG−Fe(II)TauD, these samples were mixed with O_2-saturated buffer in the stopped-flow apparatus (Figure 5). As shown in panel A, 500 μM αKG−Fe(II)TauD reacted slowly with ~350 μM oxygen (assuming that the 250 μM dithionite reacted immediately with an equivalent concentration of O_2 that was initially

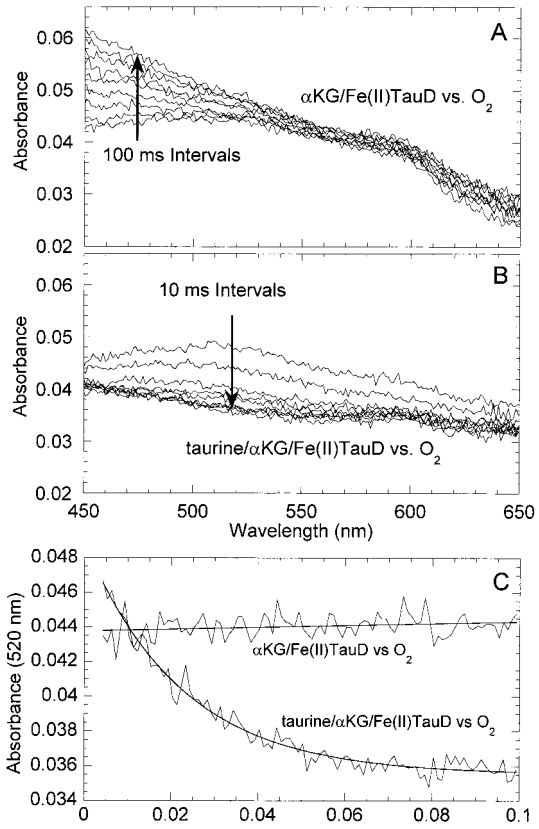

FIGURE 5: Rate of oxygen interaction with αKG−Fe(II)TauD and taurine−αKG−Fe(II)TauD using stopped-flow spectroscopy. (A) Spectra derived from mixing αKG−Fe(II)TauD [4 mM αKG, 1 mM Fe(II), 1 mM TauD, and 0.5 mM dithionite] with oxygen-saturated (1.2 mM) buffer. The least intense spectrum was recorded at 7 ms, and the spectra with increasing intensities were obtained at 100 ms intervals. (B) Absorption spectra derived from mixing taurine−αKG−Fe(II)TauD [4 mM αKG, 4 mM taurine, 1 mM Fe(II), 1 mM TauD, and 0.5 mM dithionite] with oxygen-saturated buffer (1.2 mM). After mixing (7 ms), the spectra with decreasing intensities were obtained at 10 ms intervals. (C) Comparison of the change in 520 nm absorbance when αKG−Fe(II)TauD or taurine−αKG−Fe(II)TauD was reacted with oxygen. During the initial 100 ms, almost no change in absorption was detected when αKG−Fe(II)TauD was reacted with oxygen. The data for taurine−αKG−Fe(II)TauD reacting with oxygen were fit to a single-exponential decay, yielding a rate of 42 ± 9 s^{-1}.

present at 600 μM) to generate an increase in absorbance below ~500 nm; however, the absorption associated with αKG−Fe(II)TauD (between 520 and 640 nm) remained relatively constant. Experiments carried out in the absence of protein suggested that the increase in absorbance below 500 nm was associated with the oxidation of Fe(II) to Fe(III). In contrast to this slow event, rapid changes were seen when 500 μM taurine−αKG−Fe(II)TauD was reacted with ~350 μM oxygen as shown in panel B. Within 70 ms, the absorption attributed to the taurine−αKG−Fe(II)TauD state (between 530 and 640 nm) decreased in intensity to a minimum value. The rates of 520 nm absorption changes for the two species are compared in panel C. Whereas no change in intensity was observed for the first 100 ms for a sample lacking taurine, the spectrum attributed to taurine−αKG−Fe(II)TauD was able to be fit to a single-exponential process with a rate of 42 ± 9 s^{-1}. Experiments were also carried out where 500 μM αKG−Fe(II)TauD or 500 μM taurine−αKG−Fe(II)TauD was reacted with ~550 μM oxygen. Again, the spectrum attributed to taurine−αKG−Fe(II)TauD could be fit to a single-exponential process (34 ± 12 s^{-1}), whereas the sample lacking taurine was relatively unchanged during the first 100 ms of the reaction.

DISCUSSION

We have used equilibrium and stopped-flow UV−visible spectroscopic approaches to examine the interactions of TauD with Fe(II), αKG, and taurine. These results are discussed in the context of current models for cosubstrate binding to αKG-dependent hydroxylases or related enzymes, and integrated into a preliminary kinetic model for TauD catalysis.

Origin of the TauD Spectra. The spectra associated with αKG−Fe(II)TauD and taurine−αKG−Fe(II)TauD are likely to arise from subtle perturbation of the same underlying chromophore. On the basis of literature precedents involving Fe(II) model compound studies (*21*−*25*), MCD experiments with CS (*13*, *14*), and structural elucidation of DAOCS with αKG bound (*15*), we attribute the TauD-related spectra to low-lying metal-to-ligand charge-transfer transitions arising from chelation of Fe(II) by the C-1 carboxylate and C-2 keto groups of αKG. The TauD-associated spectra, with an absorption maximum at 530 nm (ϵ = 140 M^{-1} cm^{-1}) or 520 nm (ϵ = 180 M^{-1} cm^{-1}) and shoulders at 470 and 570 nm, closely resemble those reported for benzoylformate complexes of Fe(II) (*21*−*25*). Depending on the ligand framework, these complexes exhibit absorption maxima ranging from 531 to 555 nm with extinction coefficients ranging from 280 to 690 M^{-1} cm^{-1}. For example, the complex derived from the hydrotris(3,5-diphenylpyrazol-1-yl)borate tripodal ligand exhibits maximal absorption at 531 nm (ϵ = 340 M^{-1} cm^{-1}) with shoulders at 476 nm (210 M^{-1} cm^{-1}) and 584 nm (300 M^{-1} cm^{-1}) (*25*). The structure of this biomimetric complex reveals the presence of five-coordinate Fe(II) in a trigonal bipyramidyl environment with the benzoylformate carboxylate bound in the equatorial plane and the α-keto group coordinated at an apical position. In other complexes (*21*, *22*), Fe(II) is six-coordinate with both the carboxylate and α-keto group bound in the equatorial plane. Likewise, a six-coordinate structure has been proposed for CS in the presence of αKG on the basis of MCD studies (*13*). Like the model compounds and TauD, this protein exhibits an absorption at 500 nm (ϵ = 375 M^{-1} cm^{-1}). The CS MCD spectrum is further perturbed upon addition of the cosubstrate, deoxyguanidinoproclavaminic acid, and this result was interpreted as a shift to a five-coordinate geometry with the αKG still bound in a chelating mode. Direct evidence for αKG chelation of Fe(II) in a αKG-dependent dioxygenase was obtained for DAOCS (*15*). The crystal structure of the substrate-free enzyme reveals a six-coordinate Fe(II) site with three solvent molecules, an Asp, and two His residues as ligands. Binding of αKG was shown to displace two of the water molecules, and the substrate was observed to bind to the enzyme metallocenter via its carbonyl and C-1 carboxylate groups. We propose that the αKG−Fe(II)TauD absorption spectrum arises from this consensus coordination model, and suggest that this UV−visible signature is diagnostic of the αKG-bound state of this class of enzymes. For example, an analogous spectrum was recently observed for αKG−Fe(II)TfdA.[3]

The presence of taurine perturbs the spectrum associated with αKG−Fe(II)TauD, but the chelate binding mode of

αKG is retained. The spectral perturbation is fairly specific for taurine as demonstrated by the absence of a similar transition when using 2-aminoethylphosphonate (where the taurine sulfur is replaced with a phosphorus) or *N*-phenyltaurine. Thus, it appears that both the sulfonate and amino groups are critical for proper binding of this substrate. We have no evidence supporting or opposing direct taurine coordination to the metal center; however, MCD studies on CS (*13*) suggest the loss of a coordinating ligand upon substrate binding to this mechanistically related enzyme. Similarly, substrate binding to IPNS creates a five-coordinate Fe(II) site to which oxygen (or the oxygen analogue nitric oxide) can bind (*16*). Moreover, many of the substrates for members of the αKG-dependent dioxygenase superfamily are unlikely to be capable of binding to Fe(II). Catalytic activity likely requires that Fe(II) be able to coordinate oxygen, so the loss of a metal ligand to allow oxygen coordination is quite reasonable, whereas the binding of a second substrate to the metal is counterintuitive. On the basis of this analysis, we suggest that direct coordination of taurine seems unlikely and propose that taurine binds near the metal site. Substrate binding results in absorption changes, perhaps due to a change in the ligation of the Fe(II) center from six-coordinate to five-coordinate. Nearly identical spectral changes were observed upon 2,4-D binding to αKG−Fe(II)TfdA.[3]

The α-keto acid specificity of TauD chromophore formation provides insight into possible cooperative binding effects and geometrical constraints of the active site. Incubation of Fe(II)TauD with α-ketoadipate led to barely detectable absorption at 530 nm, whereas the further inclusion of taurine led to 18% of the 520 nm absorption observed in the case of αKG. A similar, but less marked, effect is seen in the case of α-ketocaproate (8%). In contrast, no absorption was observed in this region of the spectrum for α-ketoisovalerate or pyruvate, even when these molecules were present in 20-fold molar excess over protein. On the basis of the inability of α-ketoisovalerate or pyruvate to support enzyme activity and their inability to produce the αKG-like chromophore, we suggest that these α-keto acids do not bind to Fe(II)-TauD in a productive, chelated manner. The presence of taurine appears to constrain the possible binding modes of α-ketoadipate and α-ketocaproate as evidenced by the enhanced absorption. Direct interactions (e.g., electrostatic or hydrogen bonding) between the cosubstrates may play a role in stabilizing the α-keto acid−Fe(II)TauD chromophore. These types of direct interactions might be expected since during catalysis a single oxygen atom is incorporated into each cosubstrate. Support for an α-keto acid-bound state with alternative chromophoric properties is available from model studies (*22*, *25*). Substitution of pyruvate or phenylpyruvate for benzoylformate in two of the model compounds mentioned earlier led to dramatic reductions in absorption intensities and shifts to lower wavelengths for the maxima.

Stoichiometry of Fe(II), αKG, and Taurine Binding to TauD. Analysis of UV−visible spectroscopic changes associated with TauD in the presence of varied concentrations of Fe(II), αKG, and taurine yielded the expected 1/1 stoichiometries for binding these reagents. The studies also revealed that taurine markedly enhanced the binding of αKG to TauD, changing the K_d from approximately 270 to ∼20 μM. The ability of taurine to increase the affinity of TauD for αKG could arise through protein conformational changes. It is also possible, however, that the two substrates interact directly. For example, the taurine amino group may associate with the C-5 carboxylate group of αKG by electrostatic or hydrogen bonding interactions. Similiar direct interactions between taurine and α-ketoadipate could account for the detection of the taurine−α-ketoadipate−Fe(II)TauD chromophore.

Rates of αKG−Fe(II)TauD and Taurine−αKG−Fe(II)-TauD Chromophore Formation. The measured rates of formation of the αKG−Fe(II)TauD and αKG−taurine−Fe(II)TauD chromophores (both about 40 s^{-1}) and of taurine binding to αKG−Fe(II)TauD (>140 s^{-1}) establish that these spectral changes could reflect mechanistically relevant transitions (for comparison, the turnover number for TauD was calculated to be 2 s^{-1}). Because the rate of chromophore formation was independent of the substrate or protein concentration, the measured rates do not represent the rates of αKG binding to protein. Rather, the zero-order process is likely to represent a conformational change at the αKG-bound active site. We speculate that αKG rapidly binds to Fe(II)TauD in a nonchromophoric fashion (possibly binding to the metal center with a single oxygen atom), and the observed rate reflects formation of the Fe(II)-chelated species.

Oxygen Reactivity of αKG−Fe(II)TauD and αKG−Taurine−Fe(II)TauD. The chromophore associated with taurine−αKG−Fe(II)TauD decayed rapidly (42 s^{-1}) in the presence of oxygen, whereas the absorption due to αKG−Fe(II)TauD was relatively unaffected by oxygen exposure. On the basis of these reactivity differences, we propose that TauD has evolved to preferentially bind oxygen only in the presence of both cosubstrates. This situation would reduce the incidence of nonproductive oxidation reactions that could lead to enzyme inactivation. Uncoupled reactions, in which αKG decomposes to CO_2 and succinate without concomitant substrate hydroxylation, have been observed for several αKG-dependent dioxygenases (*26*−*28*). These reactions lead to enzyme inactivation, although ascorbic acid can partially restore the activity. The TauD reaction rate is linear for several minutes in the absence of ascorbic acid, consistent with a lack of significant uncoupling. Furthermore, the closely related enzyme TfdA has been shown to be tightly coupled when decomposing 2,4-D (*29*), although it too undergoes oxidative inactivation with poor substrates (*28*). The enhanced reactivity of taurine−αKG−Fe(II)TauD toward oxygen is likely to arise from the creation of an oxygen-binding site on the metal center, although the possibility of O_2 binding adjacent to an activated substrate molecule cannot be excluded. We prefer a model involving direct metal−oxygen interactions for several reasons. The binding of anionic ligands to Fe(II) is expected to affect the redox potential of the metal to enhance oxygen reactivity (*20*), and a similar argument can be made for substrate binding near the metal. Furthermore, MCD spectroscopic evidence is consistent with the Fe(II) site of CS undergoing a coordination change to form a five-coordinate structure in the presence of both of its substrates, thus exposing a coordination site for oxygen binding (*14*). Structural evidence is consistent with a similar phenomenon occurring in IPNS (*16*). In that case, NO was

[3] E. L. Hegg, A. K. Whiting, R. E. Saari, J. McCracken, R. P. Hausinger, and L. Que, Jr. (1999) *Biochemistry* (in press).

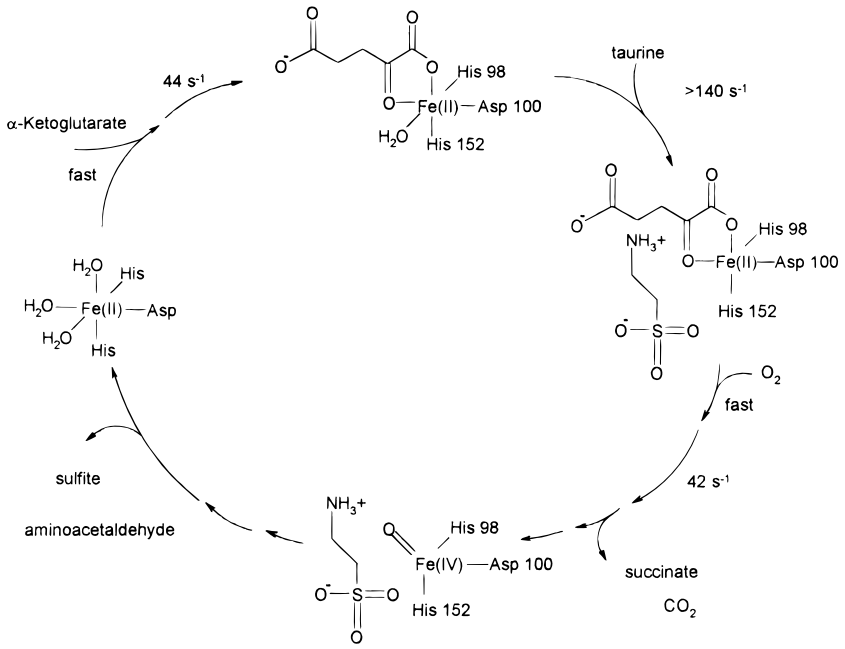

FIGURE 6: Preliminary kinetic model of TauD catalysis. The model suggests that Fe(II)TauD rapidly binds αKG to yield a nonchromophoric species. Subsequent development of the αKG−Fe(II)TauD spectrum (44 s^{-1}) is proposed to be associated with chelate binding of αKG to Fe(II). The αKG−Fe(II)TauD species binds taurine at a rate too rapid to be measured (>140 s^{-1}) in the 7 ms dead time of the instrument. The metal site in the resulting taurine−αKG−Fe(II)TauD species is proposed to be five-coordinate, based on analogy to CS (*14*). Taurine is depicted to bind near to, but not directly coordinating, the metallocenter; however, this hypothesis must be subjected to experimental testing. Oxygen binds rapidly to taurine−αKG−Fe(II)TauD and in a subsequent reaction bleaches the spectrum (42 s^{-1}). The resulting species likely gives rise to the putative Fe(IV)═O intermediate that catalyzes oxygen insertion chemistry.

shown to bind to an open site on the Fe(II) center created upon substrate binding. Model compound chemistry is also consistent with creation of an O_2 binding site on the metal. While six-coordinate Fe(II) complexes containing α-keto acid ligands are relatively unreactive (*21*, *22*), five-coordinate Fe(II) complexes are effective mimics of the αKG-dependent dioxygenases (*24*, *25*).

Kinetic Model of TauD Catalysis. In Figure 6, we integrate our equilibrium and kinetic spectroscopic results of TauD with results from other enzyme studies and relevant model chemistry. Resting state enzyme is proposed to bind Fe(II) via a 2-His-1-carboxylate facial triad (*8*, *20*), as known to be the case for other members of the enzyme superfamily (*14*, *15*). Fe(II)TauD is shown to very rapidly bind αKG in a reaction that cannot be monitored by UV−visible spectroscopy. The nonchromophoric αKG-bound state converts to the chelated species associated with the αKG−Fe(II)TauD spectrum at a rate of 44 s^{-1}. Subsequent binding of taurine is too rapid to measure. Our spectroscopic results do not rule out the possibility that taurine can bind prior to αKG [taurine−Fe(II)TauD is nonchromophoric], but we note that development of the taurine−αKG−Fe(II)TauD chromophore is essentially identical in rate (42 s^{-1}) to that seen for forming the αKG-chelated species and likely arises from the same process. The taurine−αKG−Fe(II)TauD species is suggested to possess five-coordinate Fe where the taurine is bound near the metal center, but further studies are necessary to test this proposal. Figure 6 also shows that the absorbance associated with taurine−αKG−Fe(II)TauD rapidly disappears (42 s^{-1}) when this species reacts with oxygen. Since the monitored absorbance reflects the bidentate mode of binding of αKG to the metallocenter, this rate reflects the loss of these interactions and does not necessarily reflect the rate of formation of the putative Fe(IV)═O intermediate (*20*, *30*). Consistent with chromophore bleaching reflecting an internal event, rather than O_2 binding, the disappearance of the taurine−αKG−Fe(II)TauD spectrum was unchanged when a substoichiometric amount (350 μM) or a slight excess (550 μM) of oxygen was reacted with taurine−αKG−Fe(II)TauD (500 μM). The preliminary kinetic model shown in Figure 6 should be viewed as a working hypothesis to stimulate future efforts to characterize TauD and other members of the αKG-dependent dioxygenase superfamily.

ACKNOWLEDGMENT

We thank Thomas Leisinger for kindly providing plasmid pME4141, Shelagh Ferguson-Miller and Denise Mills for use of the stopped-flow instrument and assistance with its operation, and Larry Que, Julie Dunning, Debbie Hogan, Gerry Colpas, Tommy Auchtung, and an anonymous reviewer for helpful comments on the manuscript.

REFERENCES

1. Eichhorn, E., van der Ploeg, J. R., Kertesz, M. A., and Leisinger, T. (1997) *J. Biol. Chem. 272*, 23031−23036.
2. van der Ploeg, J. R., Weiss, M. A., Saller, E., Nashimoto, H., Saito, N., Kertesz, M. A., and Leisinger, T. (1996) *J. Bacteriol. 178*, 5438−5446.
3. Chesney, R. W. (1985) *Adv. Pediatr. 32*, 1−42.
4. Jacobsen, J. G., and Smith, L. H. (1968) *Physiol. Rev. 48*, 424−511.
5. Autry, A. R., and Fitzgerald, J. W. (1990) *Biol. Fertil. Soils 10*, 50−56.
6. Fukumori, F., and Hausinger, R. P. (1993) *J. Bacteriol. 175*, 2083−2086.
7. Prescott, A. G., and John, P. (1996) *Annu. Rev. Plant Physiol. Plant Mol. Biol. 47*, 245−271.
8. Que, L., Jr., and Ho, R. Y. N. (1996) *Chem. Rev. 96*, 2607−2624.

9. Kivirikko, K. I., and Pihlajaniemi, T. (1998) *Adv. Enzymol. Relat. Areas Mol. Biol. 72*, 325−398.
10. Pirskanen, A., Kaimio, A.-M., Myllyla, R., and Kivirikko, K. I. (1996) *J. Biol. Chem. 271*, 9398−9402.
11. Lukacin, R., and Britsch, L. (1997) *Eur. J. Biochem. 249*, 748−757.
12. McGinnis, K., Ku, G. M., VanDusen, W. J., Fu, J., Garsky, V., Stern, A. M., and Friedman, P. A. (1996) *Biochemistry 35*, 3957−3962.
13. Pavel, E. G., Zhou, J., Busby, R. W., Gunsior, M., Townsend, C. A., and Solomon, E. I. (1998) *J. Am. Chem. Soc. 120*, 743−753.
14. Zhou, J., Gunsior, M., Bachmann, B. O., Townsend, C. A., and Solomon, E. I. (1998) *J. Am. Chem. Soc. 120*, 13539−13540.
15. Valegård, K., van Scheltinga, A. C. T., Lloyd, M. D., Hara, T., Ramaswamy, S., Perrakis, A., Thompson, A., Lee, H.-S., Baldwin, J. E., Schofield, C. J., Hajdu, J., and Andersson, I. (1998) *Nature 394*, 805−809.
16. Roach, P. L., Clifton, I. J., Hensgens, C. M. H., Shibata, N., Schofield, C. J., Hajdu, J., and Baldwin, J. E. (1997) *Nature 387*, 827−830.
17. Borovok, I., Landman, O., Kreisberg-Zakarin, R., Aharonowitz, Y., and Cohen, G. (1996) *Biochemistry 35*, 1981−1987.
18. Myllyharju, J., and Kivirikko, K. I. (1997) *EMBO J. 16*, 1173−1180.
19. Lamberg, A., Pihlajaniemi, T., and Kivirikko, K. I. (1995) *J. Biol. Chem. 270*, 9926−9931.
20. Hegg, E. L., and Que, L., Jr. (1997) *Eur. J. Biochem. 250*, 625−629.
21. Chiou, Y.-M., and Que, L., Jr. (1992) *J. Am. Chem. Soc. 114*, 7567−7568.
22. Chiou, Y.-M., and Que, L., Jr. (1995) *J. Am. Chem. Soc. 117*, 3999−4013.
23. Hikichi, S., Ogihara, T., Fujisawa, K., Kitajima, N., Akita, M., and Moro-oka, Y. (1997) *Inorg. Chem. 36*, 4539−4547.
24. Ha, E. H., Ho, R. Y. N., Kisiel, J. F., and Valentine, J. S. (1995) *Inorg. Chem. 34*, 2265−2266.
25. Hegg, E. L., Ho, R. Y. N., and Que, L., Jr. (1999) *J. Am. Chem. Soc. 121*, 1972−1973.
26. Tuderman, L., Myllyla, R., and Kivirikko, K. I. (1977) *Eur. J. Biochem. 80*, 341−348.
27. Counts, D. F., Cardinale, G. J., and Udenfriend, S. (1978) *Proc. Natl. Acad. Sci. U.S.A. 75*, 2145−2149.
28. Saari, R. E., and Hausinger, R. P. (1998) *Biochemistry 37*, 3035−3042.
29. Fukumori, F., and Hausinger, R. P. (1993) *J. Biol. Chem. 268*, 24311−24317.
30. Hanauske-Abel, H. M., and Gunzler, V. (1982) *J. Theor. Biol. 94*, 421−455.

BI9912746